Excitations in laminar domain systems in ferroelectrics

1990 J. Phys.: Condens. Matter 2 9577

(http://iopscience.iop.org/0953-8984/2/48/011)

J. Phys.: Condens. Matter **2** (1990) 9577–9588. Printed in the UK

Excitations in laminar domain systems in ferroelectrics

Li Xingjiao†, Li Yibing†, Li Shaoping‡, L E Cross‡ and R E Newnham‡

† Department of Solid State Electronics, Huazhong University of Science and Technology, Wuhan 430074, People's Republic of China

‡ Materials Research Laboratory, Pennsylvania University, University Park, PA 16801, USA

Received 23 January 1990, in final form 13 July 1990

Abstract. Electroacoustic waves are investigated in the 180° periodic domain structure. Some elementary methods are provided. The expressions for the Hamiltonian and the explicit equations for the dispersion of bulk modes as well as interface modes are obtained. The results are analysed and a possible elementary mode is proposed.

1. Introduction

Since Bleustein [1] and Gulyaev [2] discussed a new type of surface wave in piezoelectric crystals, many researchers have done much work in the field. Maerfeld and Tournois [3] published a paper about the study of the electroacoustic waves of the ferroelectric domain wall. One of the present authors has extended the research to the case of domain-layered structure [4]. The results have been demonstrated experimentally [5]. Recently we have further extended our work to the structure of a coherent array of domains [6] and it is found that a velocity band exists. However, in the previous paper, only the interface modes were investigated. In this paper, we develop a systematic investigation of interface and bulk modes by using a new method which may be called the state combination method. A series of dispersion bands are found. An expression for the Hamiltonian of the system is given. It turns out that the modes are those of the propagation of the coupling between the displacement and the electric field. They comprise a new kind of elementary mode which exists in ferroelectric domains.

The interest in surface and interface properties of condensed media and of thin layer properties has been greatly increased at the present time owing to the possibility of fabricating layered structures by modern crystal growth techniques. The surface phonons and elementary excitations in the superlattice are of much current interest. Camley *et al* [7] have systematically investigated the propagation of transverse elastic waves in the superlattice in detail. Dobrzynski and co-workers [8, 9] have investigated surface phonons and magnons in the superlattice of two or more materials [10] by using the interface response theory. Barch *et al* [11] propose that 'dyadons' exist in the coherent array of a twin boundary; the frequency is about $10^{10}\,s^{-1}$ which involves a quasi-macromotion. A superlattice made of antiphase domains has been reported [12] and its application in acoustic transducers has been investigated [13]. It is well known that

0953-8984/90/489577 + 12 $03.50

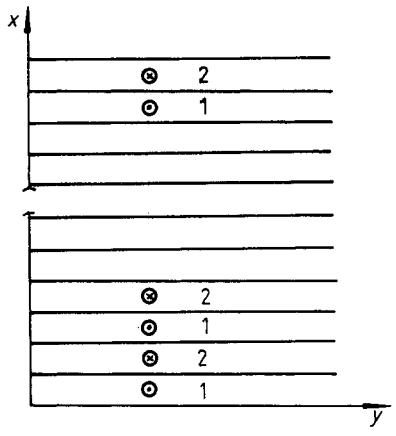

Figure 1. The orientation of domains and the co-ordination system. There are $2N$ layers. The polarization of type 1 is parallel to the z direction, while that of type 2 is opposite to the z direction.

acoustic phonons play an important role in the understanding of many physical processes, especially at low temperatures. The antiphase domain superlattice has been observed in a high-temperature superconductor [14]. We hope the present investigations may give some insight into the vibration modes in these structures. Section 2 gives the conventional method for describing the vibrations in a superlattice from which eigenvalues and eigenvectors can be found. Yet the computations are complicated. In sections 3 and 4, two other methods are introduced: the Hamiltonian function and state combinations. In section 3, we have given only general results without further computation. The emphasis in this section is on the idea of the splitting of energy of the system, while in section 4 we have derived the appropriate dispersion relations in a closed analytical form; thus the whole vibrations picture has been presented. The conclusions reached on the basis of the work described in this paper are presented in section 5.

2. Theory

The propagation of elastic waves in a piezoelectric crystal is governed by the following equations [15]:

$$\rho(\partial^2 u_i/\partial t^2) - C_{ijkl}[\partial^2 u_k/(\partial x_l\,\partial x_k)] - e_{kij}[\partial^2 \varphi/(\partial x_k\,\partial x_j)] = 0 \tag{1}$$

$$e_{jkl}[\partial^2 u_k/(\partial x_l\,\partial x_j)] - \varepsilon_{jk}[\partial^2 \varphi/(\partial x_k\,\partial x_j)] = 0 \qquad (i,j,k,l = 1,2,3) \tag{2}$$

where ρ, C_{ijkl}, e_{kjl} and ε_{jk} are the mass density, the elastic stiffness tensor, the piezoelectric tensor and the dielectric permittivity tensor, respectively. u is the displacement vector and φ the electric potential.

We assume that the layers in the superlattice belong to the 6mm class with their C axis along the z axis of a reference basis set, while the normal to the layers is x and the wavevector $\boldsymbol{k}$ is parallel to the layers, oriented along y. As shown in figure 1, the polarization of type 1 is parallel to the z direction, while polarization of type 2 is opposite to the z direction.

For each layer, we can assume the following solutions:

$$u_3 = u_n(\alpha, x)\exp[\mathrm{j}(k_y y - \omega t)] \qquad (n = 1,2,\ldots,2N) \tag{3}$$

$$\varphi = \varphi_n(\alpha, x)\exp[\mathrm{j}(k_y y - \omega t)] \qquad (n = 1,2,\ldots,2N) \tag{4}$$

where the index n indicates the cell number in the superlattice and α refers to the two constituents with $\alpha = 1, 2$. With the symmetry of our problem, the Bleustein–Gulyaev wave decouples from sagittal elastic waves. For a shear horizontal wave which we are interested in in this paper, the coupled variables (u_3, φ) can be written as

$$u_n(\alpha, x) = F_{1n} \exp(kbx) + F_{2n} \exp(-kbx) \tag{5}$$

$$\varphi_n(\alpha, x) = \pm F_{1n} \exp(kbx) \pm F_{2n} \exp(-kbx) \pm F_{3n} \exp(kx) \pm F_{4n} \exp(-kx) \tag{6}$$

where the upper sign is for $\alpha = 1$ and the lower for $\alpha = 2$;

$$b = (1 - v^2/v_T^2)^{1/2} \qquad v_T^2 = c_{44}^D/\rho \qquad c_{44}^D = c_{44} + e_{15}^2/\varepsilon_{\|}.$$

Define a four-component column vector

$$\boldsymbol{U}_n = \begin{bmatrix} D_n \\ \tau_n \\ \varphi_n \\ u_n \end{bmatrix} = \begin{bmatrix} q_n \\ p_n \end{bmatrix} \exp[\mathrm{j}(k_y y - \omega t)] \qquad \boldsymbol{F}_n = \begin{bmatrix} F_{1n} \\ F_{2n} \\ F_{3n} \\ F_{4n} \end{bmatrix} \tag{7}$$

where τ and D are the sagittal shear stress and normal component of the electrical displacement, respectively. We may call $\boldsymbol{U}$ the state vector for it must be continuous at each boundary.

The above τ_n and D are expressed as

$$\tau_n(\alpha, x) = F_{1n} \exp(kbx) - F_{2n} \exp(-kbx) + rF_{3n} \exp(kx) - rF_{4n} \exp(-kx) \tag{8}$$

$$D_n(\alpha, x) = \mp F_{3n} \exp(kx) \pm F_{4n} \exp(-kx) \tag{9}$$

where the upper sign is for $\alpha = 1$ and the lower for $\alpha = 2$; $r = b_{MT}/b$ and $b_{MT} = e_{15}^2/\varepsilon_{11} c_{44}^D$. It is convenient to assume that the variable x appearing in equations (5), (6), (8) and (9) is a local variable ranging from 0 to h in each layer. Therefore for each layer we have

$$\boldsymbol{U}_n(1, x) = \mathbf{G}(1, x)\boldsymbol{F}_n \qquad \boldsymbol{U}_m(2, x) = \mathbf{G}(2, x)\boldsymbol{F}_m \tag{10}$$

where

$$\mathbf{G}(p, x) = \begin{bmatrix} 0 & 0 & \mp\exp(kx) & \pm\exp(-kx) \\ \exp(kbx) & -\exp(-kbx) & r\exp(kx) & -r\exp(-kx) \\ \pm\exp(kbx) & \pm\exp(-kbx) & \pm\exp(kx) & \pm\exp(-kx) \\ \exp(kbx) & \exp(-kbx) & 0 & 0 \end{bmatrix}$$

and the upper sign is for $\alpha = 1$ and the lower for $\alpha = 2$.

From the boundary conditions at the interface, we have (see appendix 1)

$$F_{2N} = [\mathbf{G}^{-1}(2,0)\mathbf{G}(1,h)\mathbf{G}^{-1}(1,0)\mathbf{G}(2,h)]^N F_{2N}. \tag{11}$$

After some manipulations (see appendix 1), the dispersion equations were obtained:

$$|\mathbf{T} - \exp(\mathrm{j}2\pi l/N)E| = 0 \tag{12}$$

where $\mathbf{T} = \mathbf{G}^{-1}(2,0)\mathbf{G}(1,h)\mathbf{G}^{-1}(1,0)\mathbf{G}(2,h)$, $\mathbf{T}$ is the transfer matrix. $\mathbf{E}$ is a 4×4 unit matrix.

3. The periodic Hamiltonian

In this section we have derived the Hamiltonian function of the system, which is another way of describing the vibrations of the ferroelectric domains. From [16], we have a periodic Hamiltonian of the system with the Hamiltonian function given by

$$H = \tfrac{1}{2}[q_n^*(\alpha,x)P(\alpha,x)q_n(\alpha,x) + p_n^*(\alpha,x)Q(\alpha,x)p_n(\alpha,x)] \tag{13}$$

and

$$\frac{\mathrm{d}}{\mathrm{d}x}\begin{bmatrix}\mathbf{q}_n\\ \mathbf{p}_n\end{bmatrix} = \mathbf{A}(\alpha,x)\begin{bmatrix}\mathbf{q}_n\\ \mathbf{p}_n\end{bmatrix} \qquad \mathbf{A}(\alpha,x) = \begin{bmatrix}0 & \mathbf{Q}(\alpha,x)\\ -\mathbf{P}(\alpha,x) & 0\end{bmatrix}$$

where

$$\mathbf{q}_n(\alpha,x) = \begin{bmatrix}D_n(\alpha,x)\\ \tau_n(\alpha,x)\end{bmatrix} \qquad \mathbf{p}(\alpha,x) = \begin{bmatrix}\varphi_n(\alpha,x)\\ u_n(\alpha,x)\end{bmatrix}$$

$$\mathbf{Q}(\alpha,x) = \begin{bmatrix}-\varepsilon_{11}k^2 & \pm e_{15}k^2\\ \pm e_{15}k^2 & C_{11}k^2 - \rho\omega^2\end{bmatrix}$$

$$\mathbf{P}(\alpha,x) = \begin{bmatrix}C_{44}^{\mathrm{D}}/C_{44}\varepsilon_{11} & \mp e_{15}/C_{44}^{\mathrm{D}}\varepsilon_{11}\\ \mp e_{15}^{\mathrm{D}}/C_{44}\varepsilon_{11} & -1/C_{44}^{\mathrm{D}}\end{bmatrix}$$

where the upper sign is for $\alpha = 1$ and the lower for $\alpha = 2$.

For the nth periodic layer, we have

$$D_n(\alpha,x) = \sum_{l=1}^{N} D_{n,l}(\alpha,x) = \sum_{l=1}^{N} e_{15}k\exp\left(\mathrm{j}\frac{2\pi l}{N}n\right)[\mp C_{3l}^{\alpha}\exp(kx) \pm C_{4l}^{\alpha}\exp(-kx)]$$

$$\tau_n(\alpha,x) = \sum_{l=1}^{N}\tau_{n,l}(\alpha,x) = C_{44}^{\mathrm{D}}kb\sum_{l=1}^{N}\exp\left(\mathrm{j}\frac{2\pi l}{N}n\right)$$
$$\times [C_{1l}^{\alpha}\exp(kbx) - C_{2l}^{\alpha}\exp(-kbx) + \gamma C_{3l}^{\alpha}\exp(kx) - \gamma C_{4l}^{\alpha}\exp(-kx)]$$

$$\varphi_n(\alpha,x) = \sum_{l=1}^{N}\varphi_{n,l}(\alpha,x) = \frac{e_{15}}{\varepsilon_{11}}\sum_{l=1}^{N}\exp\left(\mathrm{j}\frac{2\pi l}{N}n\right)$$
$$\times [\pm C_{1l}^{\alpha}\exp(kbx) \pm C_{2l}^{\alpha}\exp(-kbx) \pm C_{3l}^{\alpha}\exp(kx) \pm C_{4l}^{\alpha}\exp(-kx)]$$

$$u_n(\alpha, x) = \sum_{l=1}^{N} u_{n,l}(\alpha, x) = \sum_{l=1}^{N} \exp\left(\mathrm{j}\frac{2\pi l}{N} n\right) [C_{1l}^{\alpha} \exp(kbx) + C_{2l}^{\alpha} \exp(-kbx)] \tag{14}$$

where

$$\mathbf{C}_l^{\alpha} = \begin{bmatrix} A_l^{\alpha} \\ B_l^{\alpha} \end{bmatrix} = \begin{bmatrix} C_{1l}^{\alpha} \\ C_{2l}^{\alpha} \\ C_{3l}^{\alpha} \\ C_{4l}^{\alpha} \end{bmatrix} \qquad (l = 1, 2, \ldots, N)$$

stands for the vibration amplitude coefficient vector corresponding to the lth mode at the first periodic layer. Substituting equation (14) into equation (13), after some complicated algebraic computations, we obtain

$$H = \sum_{l=1}^{N} \left(\frac{(\rho\omega_l^2 - C_{44}^{\mathrm{D}} k^2)(C_{1l}^{\alpha} C_{2l}^{\alpha})}{2} - \frac{e_{15} k^2}{2\varepsilon_{11}} (C_{3l}^{\alpha} C_{4l}^{\alpha}) \right) \tag{15}$$

with $\alpha = 1, 2$ for different types of domain.

$\mathbf{C}_l^{\alpha}$ are determined by

$$[\mathbf{T}^{\alpha} - \exp(\mathrm{j}2\pi l/N)]\mathbf{C}_l^{\alpha} = 0 \tag{16}$$

where $\mathbf{T}^{\alpha}$ is the transfer matrix for type α domains:

$$\mathbf{T}^{\alpha} = \mathbf{G}^{-1}(\alpha, 0)\mathbf{G}(\alpha', h)\mathbf{G}^{-1}(\alpha', 0)\mathbf{G}(\alpha, h) \qquad (\alpha \neq \alpha';\ \alpha, \alpha' = 1, 2).$$

$\mathbf{C}_l^{\alpha}$ are the components of the normalized eigenvectors of the transfer matrix and $\exp(\mathrm{j}2\pi l/N)$ are the corresponding eigenvalues. In equation (15), C_{1l}^{α} and C_{2l}^{α} are the elastic displacement amplitudes of the lth vibration modes, and C_{3l}^{α} and C_{4l}^{α} are the electric field amplitudes of the lth vibration modes. From equation (15), we know that there exists a separate energy value corresponding to the lth vibration mode for each k, i.e. $l = 1, 2, 3, \ldots, N$; $H = H_1, H_2, H_3, \ldots, H_N$. It should be noted that, in constructing the vibration spectrum for a set of N domain layers, we have obtained N independent oscillators corresponding to N modes of the system. Each oscillator has an independent Hamiltonian energy. The Hamiltonian of the system is the sum of the energy of N independent oscillators.

4. The dispersion relations

The dispersion relations of the interface modes may be obtained from equation (12). Here we present a simple computation which leads to the solutions of both interface and bulk modes. The emphasis in this work is on obtaining results analytically as much as possible although computer calculations are ultimately required to translate these

analytical results into more easily understood plots. Equation (10) can be written in another form:

$$\mathbf{U}_n(\alpha, x) = \mathbf{M}_n(\alpha, x)\mathbf{E}_n \tag{17}$$

where

$$\mathbf{M}_n(\alpha,x) = \begin{bmatrix} -k\cosh(kx) & 0 & -k\sinh(kx) & 0 \\ \pm ke_{15}\cosh(kx) & k_x^{\mathrm{D}}C_{44}\cos(k_x x) & \pm ke_{15}\sinh(kx) & -k_x C_{44}^{\mathrm{D}}\sin(k_x x) \\ \sinh(kx) & \pm[e_{15}\sin(k_x x)]/\varepsilon_{11} & \cosh(kx) & e_{15}\cos(k_x x) \\ 0 & \sin k_x x & 0 & \cos(k_x x) \end{bmatrix}$$

$k_x^2 = (C_{44}^{\mathrm{D}})^{-1}(-C_{44}^{\mathrm{D}}k^2 + \rho\omega^2)$

for bulk modes, while for interface modes we can replace the trigonometric functions by hyperbolic functions, where x is the local variable ranging from $-h$ to h of the domain thickness $2h$.

Equation (17) may be written in the following form:

$$\mathbf{U}_n(\alpha, x) = \begin{bmatrix} \mathbf{S}_1(\alpha, x) & \mathbf{S}_2(\alpha, x) \\ \mathbf{R}_1(\alpha, x) & \mathbf{R}_2(\alpha, x) \end{bmatrix}\begin{bmatrix} C_I \\ C_J \end{bmatrix}. \tag{18}$$

Thus the above 4×4 matrix is composed of four matrices with $\mathbf{S}_1(\alpha, x)$ and $\mathbf{R}_2(\alpha, x)$ symmetrical in x while $\mathbf{S}_2(\alpha, x)$ and $\mathbf{R}_1(\alpha, x)$ are antisymmetrical. In this way we can simplify the computations which we call the state combination method.

The expressions for the 2×2 matrices of $\mathbf{S}_1(\alpha, x)$, $\mathbf{S}_2(\alpha, x)$, $\mathbf{R}_1(\alpha, x)$, $\mathbf{R}_2(\alpha, x)$ are obvious from equation (17). The boundary conditions must be satisfied in every domain boundary with

$$\mathbf{U}_n(\alpha, x)|_{x=h_1} = \mathbf{U}_{n+1}(\alpha', x)|_{x=-h_2} \tag{19}$$

while at the other boundary of the same domain

$$\mathbf{U}_n(\alpha, x)|_{x=-h_1} = \mathbf{U}_{n-1}(\alpha', x)|_{x=h_2}. \tag{20}$$

Taking into account equations (18)–(20) and the Bloch factor, for $h_1 = h_2 = h$ (the domain thickness is $2h$) we have (see appendix 2)

$$\begin{aligned} g_{11}C_I' + g_{12}\lambda C_J' &= 0 \\ g_{21}C_I' + g_{22}\lambda C_J' &= 0 \end{aligned} \tag{21}$$

where

$$g_{ij} = \mathbf{S}_i^{-1}(1, h)\mathbf{S}_j(2, h) + \mathbf{R}_i^{-1}(1, h)\mathbf{R}_j(2, h) \qquad (i, j = 1, 2)$$

with

$$\lambda = [1 + \exp(\mathrm{j}2\pi l/N)]/[1 - \exp(\mathrm{j}2\pi l/N)].$$

If, for example, $|g_{12}| \neq 0$, we have

$$|g_{21} - \lambda^2 g_{22}g_{12}^{-1}g_{11}| = 0 \tag{22}$$

while for $\lambda = 0$ we have $|g_{21}(h)| = 0$ or $|g_{12}(h)| = 0$ and for $\lambda \to \infty$ we have $|g_{22}(h)| = 0$ or $|g_{11}(h)| = 0$. In general we obtain

$$k_x \cot(2k_x h) = b_{\mathrm{MT}}k \tanh(2kh) \tag{23}$$

and

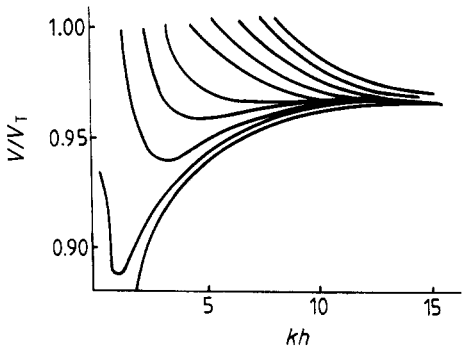

Figure 2. Phase velocity versus kh for 20-domain-layer low-lying states of the poled $BaTiO_3$ crystal ($e_{15} = 11.4\ C\ m^{-2}$; $\varepsilon_{11} = 9.87 \times 10^{-9}\ F\ m^{-1}$; $b_{MT} = 0.25$).

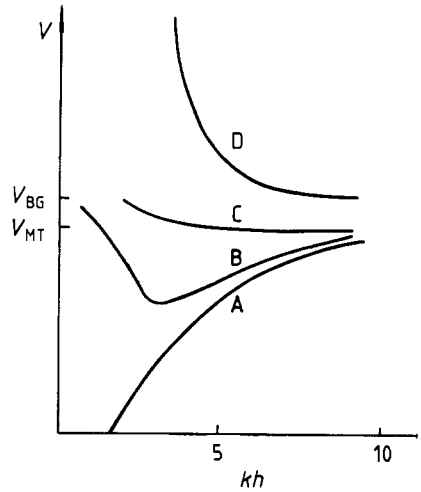

Figure 3. Four kinds of dispersion curve in a multi-layer structure.

$$k_x \cot(k_x h) = b_{MT} kc \tanh(kh) \tag{24}$$

where $b_{MT} = e_{15}^2/C_{44}^D \varepsilon_{11}$ is the limit of the bulk band:

$$b \coth(2kbh) = b_{MT} \tanh(2kh) \tag{25}$$

and

$$b \tanh(kbh) = b_{MT} \tanh(kh) \tag{26}$$

where $b = \pm(1 - v^2/v_T^2)^{1/2}$ are the upper and lower limits of the interface band.

5. Results and discussion

5.1. Characteristics of the dispersion

From equations (22)–(26), we see that some general characteristics exist:

(i) When kh is large ($kh \gg 1$), i.e. $h \gg \lambda$, the interaction between different domain walls is small. For every domain wall, we obtain the results for the MT wave. When kh is reduced from a large value, the interaction between domain walls is increased. The dispersion curve splits into N separate curves, corresponding to N vibration modes. When N is large, dispersion bands exist. In each band there are N dispersion curves corresponding to N different modes. The dispersion relations of low-lying states for $N = 10$ of the poled $BaTiO_3$ crystal are shown in figure 2. The following data are used: $e_{15} = 11.4\ C\ m^{-2}$, $v_T = 3162.21\ m\ s^{-1}$ and $b_{MT} = 0.23$.

(ii) There are four kinds of dispersion curve, as shown in figure 3. Curve A is similar to that of the flexure wave. Its dispersion curve is given by equation (26). Curve B is the same as our previous published dispersion [4]. The only difference is that here there is

a cut-off frequency. Curve C is a new kind of dispersion, which is similar to that of a Love wave. In fact, we shall call it the stiffened Love wave [15]. We should note that here the materials are the same except with opposite polarizations. The field profile analysis [6] shows that the fields of opposite domains in one period change oppositely to each other. They are 180° out of phase. Curve D is typical of the plate modes in the multi-layered structure [17]. The velocity is larger than v_T.

We have calculated the ω versus k relations from equation (22). The results are shown in figure 4. The first band is the interface mode band (see equations (25) and (26)). Its frequency lies on the right of line $v_T k$ ($v_T^2 = C_{44}^D/\rho$) on the dispersion plot of ω versus k. Along the direction normal to the interface, the exponential decrease with increasing depth of the amplitude is sinusoidally modulated. The vibration amplitude has its maximum value at each interface. The second and higher bands are bulk modes (see equations (23) and (24)). In each layer, the vibration amplitude is sinusoidally modulated. There exists a frequency gap between each band. The dispersion spectrum characteristics are similar to those obtained by Dobrzynski *et al* [8, 9]. Typical frequencies of the first and second bands are 1–10 GHz for domains of typical thickness 1 μm. Each band contains N independent vibration modes and the interface modes are the low-lying frequency states.

5.2. *Energy splitting*

From equation (15), we know that these oscillators are special phonons. They are couplings of phonons with electric polarizations in periodic 180° ferroelectric domains. There exists a splitting of the energy corresponding to the different dispersion bands and dispersion curves.

5.3. *Field profiles*

Typical field profiles are shown in figure 5. The phases of the fields on both sides of each layer change. When kh is large, only the fields near the interface are large and in the centre the electric potentials have decayed to zero. When kh is small, the amplitudes of fields (especially the electric potentials) are large in the whole medium, i.e. at the centre of the layer, the fields are comparable with those of both sides of the layer. As long-wavelength approximations are being considered, when $h \leqslant 1$ μm, we may regard the whole system as a 180° laminar domains or domain superlattice system. From the potential profiles (figure 5) we can easily get the curves of the space distribution of electric field E_x. In each layer, there is a region in which E_x is in the opposite direction and there is an interface plane of the normal components of the amplitude of the quasi-static electric field of two opposite fields [4]. For a multi-layer domain layer structure, we have div $\boldsymbol{D} = 0$ but $\oint E\,\mathrm{d}s \neq 0$, i.e. the bulk density of the free charge is zero and there exists a vibration source in the domains which leads to $\oint E\,\mathrm{d}s \neq 0$ [4].

The above theory for $h \leqslant 1$ μm is the continuum theory of the laminar domains or domain superlattice system. We propose to call these independent oscillators 'domainons' as an abbreviation of special domain vibration phonons.

We propose the following possible vibration mode. As shown in figure 6, u is the elastic displacement of the vibration mode, and E_y and E_x are the electric fields accompanying the vibration mode. u coupling with E_x and E_y travels along y direction. The dipole in the upper domain rotates counterclockwise under the force of the electric field E_y while the dipole in the lower domain rotates clockwise, thus forming a new kind

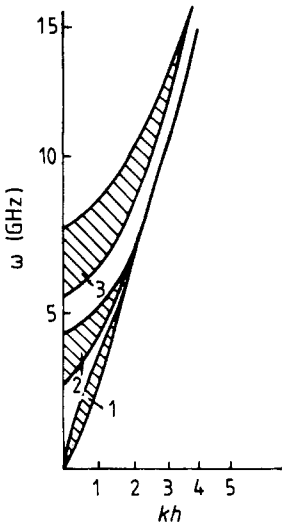

Figure 4. Dispersion bands of domain wall oscillations ($\varepsilon_{11} = 9.87 \times 10^{-9}$ F m^{-1}; $e_{15} =$ 11.4 C m^{-2}; $b_{MT} = 0.23$; $2h = 1$ μm: region 1, interface modes; regions 2 and 3, bulk modes).

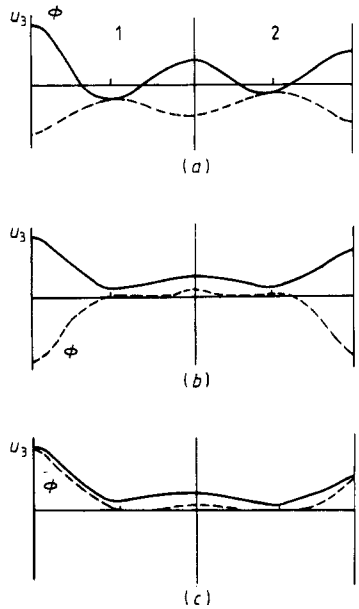

Figure 5. The displacement and potential profiles along the thickness direction over one period of the layered structure corresponding to dispersion curve B in figure 3 for ($l = 2$) (*a*) $hk = 2.0$, (*b*) $hk = 5.0$ and (*c*) $hk = 10.0$. The vertical full lines represent the domain interface. The broken curves represent electric potential profiles.

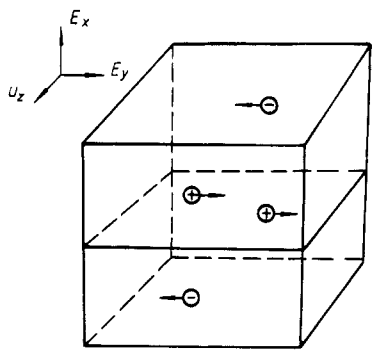

Figure 6. The possible picture of domain wall oscillations.

of mode, which is one of the characteristics of the 'domainons', i.e. the transverse vibration plus microrotation of the dipole. Its typical frequency is 10^9–10^{10} Hz. We note that in $SrTiO_3$ the soft-mode eigenvector shows [18] that the distortion consists of an out-of-phase 'rotation' of adjacent oxygen octahedra in the (100) planes. The rotation angle for the oxygen octahedra varies from 2′ at 0 K down to zero at $T_0 = 106$ K. The distortion produces domains below T_0, thus forming antiferroelectrics. As an

antiferroelectric is composed of alternating up and down dipoles, the superlattice examined in this paper consists of alternating *blocks* of up and down dipoles. This resemblance is far more than a mere superficial feature of the system. We obtained vibration modes whose eigenvectors are similar to those of antiferroelectrics. The 'domainons' differ from general acoustic phonons of the superlattice in that they relate the acoustic displacements to electric fields and are collective vibration modes of the multi-layer domains, which reflect the interactions of the whole 180° microdomain superlattice system.

Appendix 1

In the superlattice, the state vectors U in two successive layers should match each other at the interface.

At the interface of the first and second layers, $\boldsymbol{U}_1(h) = \boldsymbol{U}_2(0)$, i.e.

$$\mathbf{G}(1, h)\boldsymbol{F}_1 = \mathbf{G}(2, 0)\boldsymbol{F}_2. \tag{A1.1}$$

At the interface of the $(2i)$th layer and $(2i + 1)$th layer,

$$\mathbf{G}_{2i}(2, h)\boldsymbol{F}_{2i} = \mathbf{G}_{2i+1}(1, 0)\boldsymbol{F}_{2i+1}. \tag{A1.2}$$

At the interface of the $(2i + 1)$th and $(2i + 2)$th layer,

$$\mathbf{G}_{2i+1}(1, h)\boldsymbol{F}_{2i+1} = \mathbf{G}_{2i+2}(2, 0)\boldsymbol{F}_{2i+2}. \tag{A1.3}$$

From equations (A1.2) and (A1.3) we obtain

$$\boldsymbol{F}_{2i+2} = \mathbf{G}_{2i+2}^{-1}(2, 0)\mathbf{G}_{2i+1}(1, h)\mathbf{G}_{2i+1}^{-1}(1, 0)\mathbf{G}_{2i}(2, h)\boldsymbol{F}_{2i}. \tag{A1.4}$$

We note that the square matrices $\mathbf{G}_{2i+2}(2, 0)$, $\mathbf{G}_{2i+1}(1, h)$, etc, are all independent of the layer number; therefore

$$\begin{aligned}\boldsymbol{F}_{2N} &= [\mathbf{G}^{-1}(2, 0)\mathbf{G}(1, h)\mathbf{G}^{-1}(1, 0)\mathbf{G}(2, h)]^{N-1}\boldsymbol{F}_2 \\ &= \mathbf{T}^{N-1}\mathbf{G}^{-1}(2, 0)\mathbf{G}(1, h)\boldsymbol{F}_1\end{aligned} \tag{A1.5}$$

where $\mathbf{T} = \mathbf{G}^{-1}(2, 0)\mathbf{G}(1, h)\mathbf{G}^{-1}(1, 0)\mathbf{G}(2, h)$.

Considering that N is large, we can use the Born–Karman condition

$$\boldsymbol{U}_{2N}(h) = \boldsymbol{U}_1(0)$$

i.e.

$$\mathbf{G}_{2N}(2, h)\boldsymbol{F}_{2N} = \mathbf{G}_1(1, 0)\boldsymbol{F}_1. \tag{A1.6}$$

Substituting equation (A1.6) into equation (A1.5) we have

$$\boldsymbol{F}_{2N} = \mathbf{T}^{2N}\boldsymbol{F}_{2N}. \tag{A1.7}$$

$\boldsymbol{F}_{2N} \neq 0$; then

$$|\mathbf{T}^N - \mathbf{E}| = 0 \tag{A1.8}$$

where $\mathbf{E}$ is the 4×4 unit matrix.

Assume that

$$\mathbf{T} = \mathbf{S}^{-1}\mathbf{J}\mathbf{S} \tag{A1.9}$$

where $\mathbf{J}$ is the diagonal matrix. Combining equation (A1.9) with equation (A1.8), we obtain

$$|\mathbf{S}^{-1}\mathbf{J}^{N}\mathbf{S} - \mathbf{E}| = 0$$

i.e.

$$|\mathbf{J}^{N} - \mathbf{E}| = 0. \tag{A1.10}$$

We conclude that the diagonal matrix contains the components $\exp(\mathrm{j}2\pi l/N)$ $(l = 0, 1, 2, \ldots, N-1)$.

$$|\mathbf{J} - \exp(\mathrm{j}2\pi l/N)\mathbf{E}| = 0 \tag{A1.11}$$

and thus

$$|\mathbf{T} - \exp(\mathrm{j}2\pi l/N)\mathbf{E}| = 0. \tag{A1.12}$$

Appendix 2

For the nth layer, we have

$$\mathbf{S}_1(\alpha, x)C_I + \mathbf{S}_2(\alpha, x)C_J = q_n(\alpha, x) \tag{A2.1}$$

$$\mathbf{R}_1(\alpha, x)C_I + \mathbf{R}_2(\alpha, x)C_J = p_n(\alpha, x). \tag{A2.2}$$

Here C_I and C_J are the vibration coefficients of the nth layer.

We may set $\alpha = 1$ for the nth layer:

$$U_n(1, -h) = U_{n-1}(2, h) \tag{A2.3}$$

$$\mathbf{S}_1(1, -h)C_I + \mathbf{S}_2(1, -h)C_J = \mathbf{S}_1(2, h)C_I' + \mathbf{S}_2(2, h)C_J' \tag{A2.4}$$

$$\mathbf{R}_1(1, -h)C_I + \mathbf{R}_2(1, -h)C_J = \mathbf{R}_1(2, h)C_I' + \mathbf{R}_2(2, h)C_J'. \tag{A2.5}$$

From the symmetries of $\mathbf{S}_i(\alpha, x)$ and $\mathbf{R}_i(\alpha, x)$, we have

$$\mathbf{S}_1(1, h)C_I - \mathbf{S}_2(1, h)C_J = \mathbf{S}_1(2, h)C_I' + \mathbf{S}_2(2, h)C_J' \tag{A2.6}$$

$$-\mathbf{R}_1(1, h)C_I + \mathbf{R}_2(1, h)C_J = \mathbf{R}_1(2, h)C_I' + \mathbf{R}_2(2, h)C_J' \tag{A2.7}$$

while in the other boundary of the domain

$$U_n(1, h) = U_{n+1}(2, -h) \tag{A2.8}$$

we have

$$\mathbf{S}_1(1, h)C_I + \mathbf{S}_2(1, h)C_J = \mathbf{S}_1(2, h)C_I'' - \mathbf{S}_2(2, h)C_J'' \tag{A2.9}$$

$$\mathbf{R}_1(1, h)C_I + \mathbf{R}_2(1, h)C_J = -\mathbf{R}_1(2, h)C_I'' + \mathbf{R}_2(2, h)C_J''. \tag{A2.10}$$

For the periodic structure, the Bloch theorem may be used:

$$\begin{bmatrix} C_I'' \\ C_J'' \end{bmatrix} = \exp(\mathrm{j}2\pi l/N) \begin{bmatrix} C_I' \\ C_J' \end{bmatrix}. \tag{A2.11}$$

Thus

$$\mathbf{S}_1(1, h)C_I + \mathbf{S}_2(1, h)C_J = \exp(\mathrm{j}2\pi l/N)(\mathbf{S}_1(2, h)C_I' - \mathbf{S}_2(2, h)C_J') \tag{A2.12}$$

$$\mathbf{R}_1(1, h)C_I + \mathbf{R}_2(1, h)C_J = \exp(\mathrm{j}2\pi l/N)(-\mathbf{R}_1(2, h)C_I' + \mathbf{R}_2(2, h)C_J'). \tag{A2.13}$$

Equation (A2.6) plus equation (A2.12) gives

$$2\mathbf{S}_1(1, h)C_I = [1 + \exp(\mathrm{j}2\pi l/N)]\mathbf{S}_1(2, h)C_I' + [1 - \exp(\mathrm{j}2\pi l/N)]\mathbf{S}_2(2, h)C_J'. \tag{A2.14}$$

Equation (A2.13) minus equation (A2.7) gives

$$2\mathbf{R}_1(1,h)C_l = [1+\exp(\mathrm{j}2\pi l/N)]\mathbf{R}_1(2,h)C_l' + [1-\exp(\mathrm{j}2\pi l/N)]\mathbf{R}_2(2,h)C_l'. \tag{A2.15}$$

Combining equation (A2.14) with equation (A2.15), we have

$$[1-\exp(\mathrm{j}2\pi l/N)][\mathbf{S}_1^{-1}(1,h)\mathbf{S}_1(2,h)+\mathbf{R}_1^{-1}(1,h)\mathbf{R}_1(2,h)]C_l' + [1-\exp(\mathrm{j}2\pi l/N)]\mathbf{S}_1^{-1}(1,h)\mathbf{S}_2(2,h) + \mathbf{R}_1^{-1}(1,h)\mathbf{R}_2(2,h)]C_l' = 0. \tag{A2.16}$$

Equation (A2.12) minus equation (A2.6) and equation (A2.13) plus equation (A2.7) then combine to give

$$[1-\exp(\mathrm{j}2\pi l/N)][\mathbf{S}_2^{-1}(1,h)\mathbf{S}_1(2,h)+\mathbf{R}_2^{-1}(1,h)\mathbf{R}_1(2,h)]C_l' + [1+\exp(\mathrm{j}2\pi l/N)][\mathbf{S}_2^{-1}(1,h)\mathbf{S}_2(2,h) + \mathbf{R}_2^{-1}(1,h)\mathbf{R}_2(2,h)]C_l' = 0. \tag{A2.17}$$

Equation (A2.16) and equation (A2.17) leads to equation (21).

References

[1] Bleustein J L 1968 *Appl. Phys. Lett* **13** 412
[2] Gulyaev Y V 1969 *Sov. Phys.–JETP* **9** 63
[3] Maerfeld C and Tournois P 1971 *Appl. Phys. Lett* **19** 117
[4] Li Xingjiao 1984 *J. Appl. Phys.* **56** 88; 1987 *J. Appl. Phys.* **61** 2357
[5] Li Xingjiao, Pan W Y, Cross L E, Cao Huaze, Zhou Feng, Feng Hanhua, Li Yibing, Wu Zhiming and Wei Juan 1989 *J. Appl. Phys.* **66** 4928
[6] Li Xingjiao and Li Yibing 1990 *J. Appl. Phys.* at press
[7] Camley R E, Djafari-Rouhani B, Dobrzynski L and Maradudin A A 1983 *Phys. Rev.* B **27** 7318
[8] Dobrzynski L, Djafari-Rouhani B and Hardouin Duparc D 1984 *Phys. Rev.* B **29** 3138
[9] Dobrzynski L and Djafari-Rouhani B 1986 *Phys. Rev.* B **33** 3251
[10] Rodriguez A, Noguera A, Szawacka T, Mendinldua J and Dobrzynski L 1989 *Phys. Rev.* B **39** 12568
[11] Barch G R, Horovitz B and Krumhansl J A 1987 *Phys. Rev. Lett* **59** 1251
[12] Meeks S W and Auld B A 1985 *Appl. Phys. Lett* **47** 102
Duan F, M Nai-Ben, H Jing-Fen and W Wen-Shan 1989 *Ferroelectrics* **91** 9
[13] Zhu Y Y, Ming N B, Jiang W H and Shui Y A 1988 *Appl. Phys. Lett* **53** 1381
[14] Fung K R, Withers R L, Yan Y F and Zhao Z X 1989 *J. Phys.: Condens. Matter* **1** 317
[15] Farnell G W and Adler E L 1972 *Physics Acoustics* vol 9, ed W P Mason and R N Thurston (New York: Academic)
[16] Zinchuk L P, Dodlipenets A N and Shul'gas N A 1987 *Sov. Appl. Mech.* **24** 245
[17] Adler E L and Nassar A A 1985 *Rev. Phys. Appl.* **20** 311
[18] Scott J F 1974 *Rev. Mod. Phys.* **46** 83